2007-12-14

Thermodynamic Evidence That Ganglioside-Mediated Insertion Of Botulinum A Into The Cholinergic Nerve Ending May Precede Endocytosis And Acidification: A Langmuir Film Study

Bradley Adam Strongin
Brigham Young University - Provo

THERMODYNAMIC EVIDENCE THAT GANGLIOSIDE-MEDIATED INSERTION

OF BOTULINUM A INTO THE CHOLINERGIC NERVE ENDING MAY PRECEDE

ENDOCYTOSIS AND ACIDIFICATION: A LANGMUIR FILM STUDY

by

Bradley Adam Strongin

A thesis submitted to the faculty of

Brigham Young University

in partial fulfillment of the requirements for the degree of

Master of Science

Department of Physiology and Developmental Biology

Brigham Young University

December 2007

BRIGHAM YOUNG UNIVERSITY

GRADUATE COMMITTEE APPROVAL

of a thesis submitted by

Bradley A. Strongin

This thesis has been read by each member of the following graduate committee and by majority vote has been found to be satisfactory.

Date	David D. Busath, Chair

Date	Juliana Boerio-Goates

Date	Dixon J. Woodbury

BRIGHAM YOUNG UNIVERSITY

As chair of the candidate's graduate committee, I have read the thesis of Bradley A. Strongin in its final form and have found that (1) its format, citations, and bibliographical style are consistent and acceptable and fulfill university and department style requirements; (2) its illustrative materials including figures, tables, and charts are in place; and (3) the final manuscript is satisfactory to the graduate committee and is ready for submission to the university library.

_____   _____
Date   David D. Busath
                                         Chair, Graduate Committee

Accepted for the Department

                                         _____
                                         James P. Porter
                                         Chair, Department of Physiology
and   Developmental Biology

Accepted for the College

                                         _____
                                         Rodney J. Brown
                                         Dean, College of Life Sciences

ABSTRACT

THERMODYNAMIC EVIDENCE THAT GANGLIOSIDE-MEDIATED INSERTION OF BOTULINUM A INTO THE CHOLINERGIC NERVE ENDING MAY PRECEED ENDOCYTOSIS AND ACIDIFICATION: A LANGMUIR FILM STUDY

Bradley A. Strongin

Department of Physiology and Developmental Biology

Master of Science

Botulinum Neurotoxin (BoNT) is one of the most potent toxins known to human kind. The Atomic Force Microscope (AFM) was employed to investigate the conditions under which BoNT type A heavy chain would bind and/or insert into mica supported dipalmitoylphosphatidylcholine (DPPC) lipid bilayers. As an alternate technique, DPPC/GT1b or total ganglioside extract (80:20) monolayers of a Langmuir Blodgett (LB) Trough were adapted to be artificial membrane models for toxin insertion studies. We conclude that LB monolayer studies are a promising candidate for BoNT/A membrane insertion investigation. Botulinum neurotoxin serotype A insertions into the LB monolayers in the presence of BoNT/A low affinity ganglioside receptor alone, independent of pH. This thermodynamic evidence indicates that BoNT/A may begin its heavy chain insertion into the cholinergic nerve ending before endocytosis and acidification.

ACKNOWLEDGEMENTS

TABLE OF CONTENTS

LIST OF FIGURES AND TABLES

Introduction

Botulinum Neurotoxin (BoNT) is generally considered the most poisonous of all poisons (1,2). It is so potent that the minimum dosage needed for its toxic effects of neuroparalysis in a vulnerable cell is yet to be measured but theory projects that only one BoNT molecule may be sufficient to inactivate a nerve terminal.   Nevertheless it follows a complex multi-step pathway in order to intoxicate its target cell, the excitatory peripheral cholinergic nerve ending(2).

BoNT is now being used with and considered for a wide variety of applications. As an easily synthesized, potent and relatively stable toxin with a diverse etiology, being able to enter and infect the body through oral ingestion, inhalation, injection and wound contamination, this toxin poses as a viable candidate for bioterrorism. Kortepeter et al, from the U.S. Army Medical Research Institute of Infectious Diseases lists botulism as one of the top most dangerous bioterrorist threats (3). It is also being used to treat diseases that involve excessive cholinergic nerve ending activity, like focal, foot and axial dystonia. Therapeutically BoNT has also shown promise in treating many other ailments including strabismus, bruxism, rhinitis, and tremor (4).

Unlike many toxins, BoNT moves through the body by exploiting existing pathways, like transcytosis, that do not kill cells in the process. For this reason, fragments of BoNT are being studied as potential drug carriers for new vaccines and therapeutic drugs that can be administered orally or by inhalation (2).

Seven BoNT serotypes have been found: A,B,C,D,E,F and G. Clostridium botulinum, Clostridium baratii, and Clostridium butyricum are the three bacteria known to produce botulinum neurotoxins, with Clostridium botulinum being the most common.

All Botulinum neurotoxins (BoNTs) are translated as single polypeptide chains that must later be nicked into two chains that consist of a ~100 kDa heavy chain and a ~50 kDa light chain. The different strains of Clostridium vary in the proteolytic capability needed to produce the di-chain form, which is the active form of the toxin. Some do not even have the capability at all and therefore require exposure to exogenous proteases. However, there is some disagreement as to which strains lack this capability (2,5).

All seven serotypes are synthesized as multimeric protein complexes containing the 150 kDa toxin and other nontoxic proteins. The complex sizes are serotype specific with types E and F forming the smallest at 300 kDa, and type A forming the largest at 900 kDa (5). There is little reason to believe that the full complex makes it intact to the target cell, and experiments show that the complex dissociates from the 150 kDa toxin in pH 7.4 solution with physiologic ionic strength. It appears that the auxiliary nontoxic proteins do play an important role in protecting the toxic portion from metabolic processes, for example metabolism in the gut if the toxin has been ingested (2). Once the toxin has entered the lumen of the gut or airway it must make its way out to reach its target cell. To do this it must cross membrane barriers to enter the blood or lymph. From there, it must exit again to reach the extracellular space in the vicinity of the target cell.

The peripheral cholinergic nerve ending is BoNT's target cell. The nerve terminus is believed to be recognized by the toxin through highly specific, high affinity receptors found on the nerve ending's outer cell membrane. There has been difficulty in identifying these receptors, partially due to the challenges associated with the potency of the toxin and that peripheral nerve endings contain so little tissue (2).

Several different labs have all indicated that a sialic acid containing molecule, is

involved in reception and binding of the molecule (6,7,8,9). It has been difficult to accept a ganglioside as the specific BoNT receptor at the peripheral-neuron because it is so broadly distributed in cell membranes. Additionally, the modest affinity for ganglioside does not match well with the extreme potency of BoNTs. Finally, ganglioside as the principle receptor does not coincide with the fact that there is serotype-specific binding on the exterior of the nerve ending, as manifest by studies that have found little cross-antagonism of binding in the presence of serotypes A and B (10). To obtain selectivity and sensitivity, a two-step mechanism has been hypothesized. BoNT is assumed to bind initially to a ganglioside on the neuronal membrane. This binding is weak but sufficient to tether the toxin to the cell surface. The tethered toxin diffuses laterally until it is exposed to a more serotype-specific binding site for which it has a greater affinity.

Work is continuing forward on this issue and it has been suggested that synaptotagmin I and II are the high affinity binding receptors for BoNT serotype B (BoNT/B) (11). Synaptotagmin is a conserved integral membrane protein of the synaptic vesicles. Synaptic vesicles are neurotransmitter-containing lipid bilayer organelles found in the nerve terminus. For BoNT serotype A (BoNT/A), the most common serotype, the high affinity receptor remained illusive until recently. The synaptic vesicle protein SV2 has been identified as the missing high affinity BoNT/A receptor (12). Like synaptotagmin, SV2 is also a conserved synaptic vesicle transmembrane protein. It has been proposed (11) that once the synaptic vesicles release their neurotransmitters into the synaptic cleft by fusing with the neuronal plasma membrane, the BoNT high affinity receptors become exposed ephemerally to the toxin in the extracellular fluid. Once the toxin binds to the receptors, synaptic vesicle recycling will occur. The membrane will

involute, then bud off into the nerve ending's cytosol with the toxin trapped inside the endocytotic vesicle, as shown schematically in Figure 1b (12).

This mechanism of BoNT/A's entrance into the cholinergic nerve ending and its subsequent exit from the endosome (or endocytotic vesicle, or recycled synaptic vesicle) into the nerve ending's cytosol is highly debated in the field. This is a critical step, as its elucidation could provide the knowledge upon which BoNT/A antidotes and the path way for new highly specific cholinergic nerve pharmaceuticals could be based. Electrophysiological experiments have shown conductance increases through a vertical planar lipid bilayer once it becomes acidified. The observed current is believed to be a result of BoNT heavy chain-formed channels (13). This acid-induced pore appears to be the conduit through which the light chain leaves the vesicle and enters the cytosol. Because the current tracings persist for so long, it is assumed that the heavy chain stays in the membrane even after the light chain leaves.

A complex of three soluble N-ethylmaleimide-sensitive attachment receptor (SNARE) proteins: SNAP 25, syntaxin, and VAMP (synaptobrevin), along with other membrane and cytosolic constituents, are found in the nerve terminal. The SNARE complex is necessary for vesicle fusion and ultimately exocytosis of neurotransmitters (5). Once in the cytosol, BoNT light chain enzymatically cleaves one or more of these three proteins at a precise location, which is contingent upon the toxin serotype. This cleavage inhibits the binding and fusion of the neurotransmitter filled vesicles and thus inhibits the release of neurotransmitters into the synaptic cleft, leading to eventual complete neuroparalysis (Figure. 1b).

The pH induced translocation of the light chain endopeptidase from the endosome

is a critical step in BoNT neroparalytic activity. Multiple changes must occur in order for the light chains' successful final egress, and exposure to its substrate. The minimum changes include: heavy chain insertion into the membrane, heavy chain conformation appropriate for channel activity, light chain denaturation, exit through the heavy chain pore, and finally, breaking of the disulfide bond connecting the two chains, releasing the light chain into the nerve ending cytosol. The number of changes that require the acid environment is unknown. In this study, we seek to address the pH dependence on the initial event required for translocation, namely heavy chain insertion into the membrane. The drive to uncover these features ranges from toxin antidotes to drug design, and to furthering our understanding of neuroscience.

Furthering our repertoire of techniques will allow us to learn new aspects of BoNT and further clarify current hypotheses. Atomic Force Microscopy and Langmuir monolayers have been used in the past to successfully study peripheral proteins and even Cholera toxin. This thesis explores the candidacy of these instruments for the study of botulinum through a recently developed detoxified form of the neurotoxin.
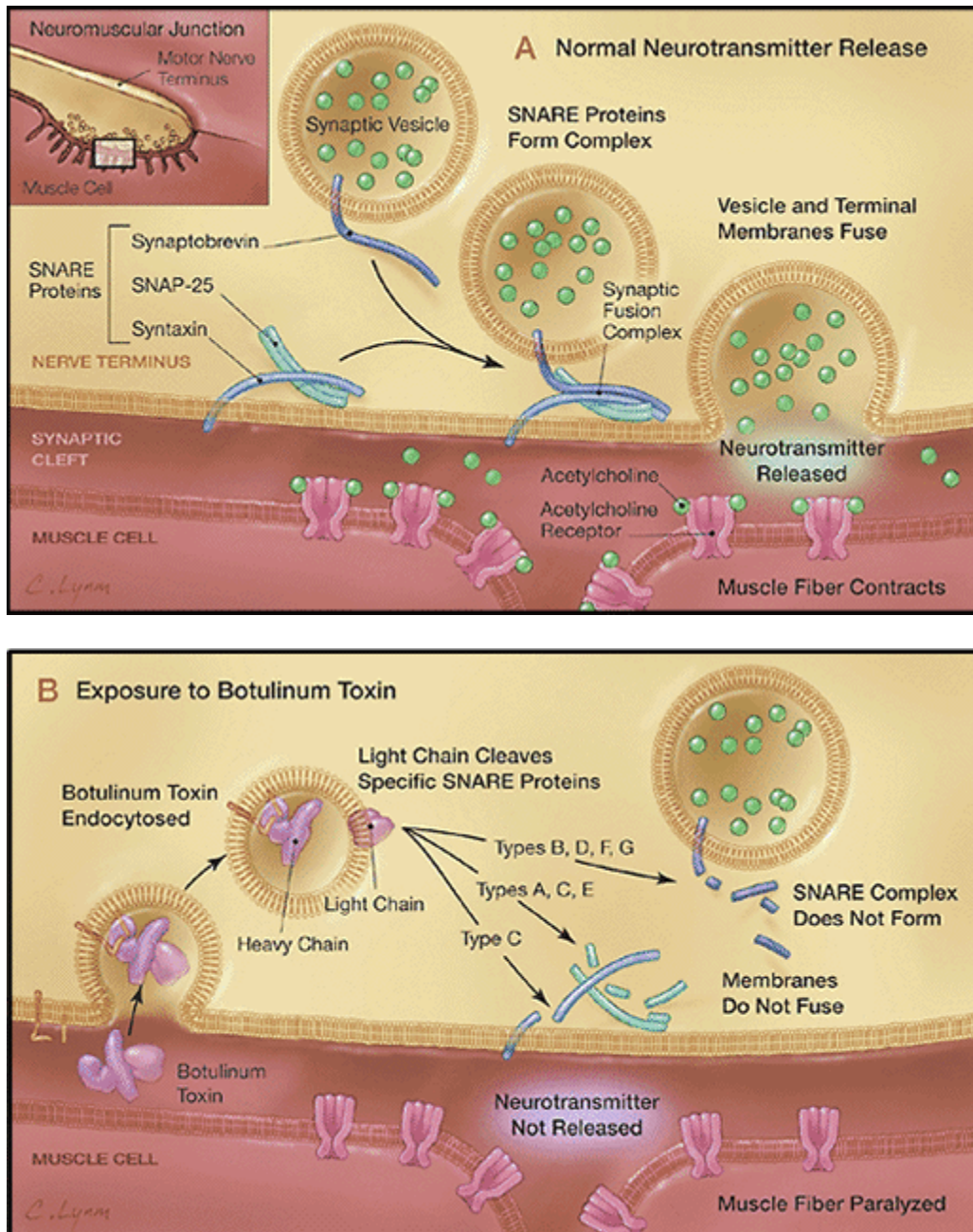
Figure 1. A Cartoon representation of normal neurotransmission at the neuromuscular junction. **B** Cartoon representation of Botulinum Neurotoxin exposure at the neuromuscular junction. Here BoNT/A is going through receptor mediated endocytosis into the peripheral cholinergic nerve, translocation of BoNT light chain from the endosome and finally enzymatic activity on the SNARE proteins according to serotype. All BoNT light chain serotype activity inhibits neurotransmition.

Materials And Methods

Atomic Force Microscopy

Both the Multimode Atomic Force Microscope (AFM) (Nanoscope IIIa Digital Instruments, Santa Barbara, CA) and the Picoscan AFM (Molecular Imaging, Phoenix, AZ) were employed. The supported lipid bilayer used for AFM investigation was composed of dipalmitoylphosphatidylcholine (DPPC) (Avanti Polar Lipids). This was deposited onto thin mica sheets (V-4 grade, Structure Probe, West Chester, PA) which are atomically flat at typical AFM scan sizes of less than fifteen micrometers. This minimizes background artifact and allows the user to better attribute the topology seen with the AFM to features of the sample being investigated and not the mica substrate. The lipid bilayer deposition was accomplished via the vesicle fusion method (14). This method in brief entails: first that DPPC is solubilized in chloroform, then the solvent is evaporated under a mild stream of nitrogen gas. After the solvent evaporates, a thin film of lipid is left behind on the glass test tube. Ultra pure water is then added to the test tube. When in lieu of pure lipid vesicles, toxin containing vesicles were desired, toxin solution instead of pure water was added. Generally the proteoliposome solution consisted of 1mg DPPC / 10mg BoNT/A heavy chain / 0.1 or 1.0 ml low ionic strength sodium phosphate buffer. The sample is vortexed to agitate the lipid from the walls of the test tube. The solution is then sonicated for about 30 seconds. The greater the time and level of sonication, the greater the homogeneity of sizes for the single unilaminar vesicles (SUV). The smaller the diameters of the SUVs, as roughly determined by the solution's

clarity ($\leq$ 200nm diameter lipid spheres are too small to scatter light), the more complete the deposition onto the mica (data not shown).

This vesicle solution was then added to a freshly cleaved mica sheet at room temperature. A minimal amount of solution was added to completely wet the mica, and allowed to sit covered for five minutes. A neutral-pH, high-ionic strength sodium phosphate buffer (between 75mM and 150mM) droplet was added to the top of the sample. The hydrophilic mica was previously bonded to an ultra-hydrophobic polyte-trafluoroethylene (PTFE) disk using a cyanoacrylate adhesive (495 Superbonder, P/N 49504, Loctite, Rocky Hill, CT) so that a relatively large droplet of buffer could be deposited to the substrate without running off (15). This was allowed to incubate for five to thirty minutes at room temperature. During the incubation time, osmosis facilitated vesicle adsorption to the mica surface.

The longer the incubation time, the more lipid was adsorbed to the mica surface. Waiting too long resulted in regions with multiple layers of lipid bilayer. Non-adsorbed free floating lipid vesicles interfered with the laser signal of the AFM. In order to remove these from the buffer droplet, the droplet was exchanged five to ten times with a pipette. After bilayer deposition, coverage was evaluated by initial AFM imaging. Near 100% lipid coverage was sought after so as to minimize the exposure of the toxin directly to the mica as it appeared to have a strong propensity to bind to the bare mica. The bilayer could be distinguished from the mica surface by measuring the depth of defects in the lipid bilayer. The bilayer was identified by a precise depth of 5nm +/- 0.5nm. The thickness of a second bilayer on top of the first was distinctly greater (16). The bilayer could also be recognized through the use of force-distance curves. This data is acquired

8

by oscillating the AFM tip vertically in the z direction starting from above the sample, and ending with a strong, graded push against the stiff mica. The varying tip force is then plotted on the y-axis, against the z position of the AFM tip on the x-axis. If a bilayer was present, the force-distance curve would show a unique tracing when the tip pushed against the lipid, resisted, and finally broke through. In the absence of lipid, pure mica will not show any break through on the force-distance graph. The lipid bilayer was robust enough to show no alterations even when a mild stream from a wash bottle was used to rinse the sample surface (data not shown).

To maintain an aqueous environment, the buffer droplet remained on the sample during AFM imaging. In order to optimize the electromagnetic interactions between the AFM silicon nitride tip and the sample, a unique, sample-dependent imaging buffer was used during imaging, ascertained by trial and error. The ionic strength of the buffer has an inverse relationship with the Debye length of the tip/sample interactions. The ion concentration was considered optimized when enough electrostatic attraction between the AFM tip and the sample allowed sample contours to be followed accurately, but without intolerable deformation of the sample. Within our spectrum of samples, the electrostatic interaction was usually attractive, and the ions of the buffer would minimize that interaction. If the salt concentration was too high, the AFM tip was difficult to keep near the surface and would not follow the contour of the sample. If the buffer's salt concentration was too low the attractive force between the tip and sample became excessive and the sample would often become deformed by the tip (17).

This aqueous environment allowed for an environment more physiological than most other ultra high resolution microscopes, such as the scanning electron microscope

9

and the transmission electron microscope, both of which require high vacuum and often an electron rich stain.

The maximum temperature attained by AFM heating within the imaging buffer was 31.2 +/- 0.5 $^{\circ}$C. as measured by a thin thermocouple (80µm diameter wires) inserted directly into the imaging droplet during AFM scanning. The liquid phase of DPPC is 41°C and higher, therefore all AFM images were obtained when DPPC was in the gel phase (18). Both the AFM's Tapping and contact modes of imaging were employed. In general, it was found that Tapping mode exerted less of a lateral pressure during scanning resulting in less deformation of the soft biological samples. AFM imaging speeds ranged from approximately 2 to 8µm/s, with line densities of 512 x 512, and typical scan areas of 0.5 to 12 µm^2.

When a proteoliposome solution containing toxin was used, its results were imaged, then a straight forward comparison to pure lipid controls was performed. However when the sample preparation had two major stages, starting with images of pure lipid vesicle fusion results and later incubating that sample with toxin, and finally scanning the outcome, additional protocol was required. After the lipid bilayer coverage was assessed, the buffer droplet was gently removed with a pipette without touching the sample's surface. An acidic buffer, of pH 4 to 5 was then added to the top of the sample. This was removed and fresh acid buffer was added a total of five times, to insure the old neutral pH buffer had been completely removed. The "flushing" process did not disturb the lipid bilayer. BoNT/A heavy chain, was then added to the acid buffer droplet to a concentration of approximately 0.2µM. This was allowed to incubate for about twenty minutes at room temperature. After the incubation process, the acid buffer was again

exchanged for the neutral pH imaging buffer. The images were then compared to the pre-toxin control images.

An alternate sample preparation to the vesicle fusion method was attempted to create high-coverage, asymmetric supported bilayer films through the Langmuir-Blodgett trough. The LB-trough is commonly used as a thin film deposition technique. This LB deposition technique allows a substrate like mica, silicon or graphite to be slowly pulled through the polar lipid monolayer resulting in deposition of a single monolayer per pass. In the case of mica, which is negatively charged when in a neutral aqueous environment, the lipid polar heads bind to the charged surface. The first pass starts in the aqueous solution, passes through the lipid monolayer, and ends in air. As a result of the first pass, the mica is coated with a single layer of lipid molecules with the polar lipid heads bound to the charged mica and the lipid tails normal to the substrate. The second pass back down into the solution deposits the second leaflet of the lipid bilayer. This happens as the mica, with the hydrophobic lipid tails oriented out, is submerged into the water and coated by a second layer of lipid. This time the lipid tails face the mica and the lipid heads are out, allowing the hydrophobic tails a minimum exposure to the water, and the polar heads a maximum exposure to the charged water-coated mica surface and the polar water bath (Figure 2).

For the attempts at BoNT/A incorporation, the lipid used for the primary layer was 1,2-dipalmitoylphospho-ethanolamine (DPPE). In order to incorporate the gangliosides into the supported bilayer exclusively in the outer leaflet, the monolayer on the LB-trough was changed between pass one and two. The second monolayer consisted of DPPC and GT1b (mole ratio of 80:20). This method resulted in better lipid coverage
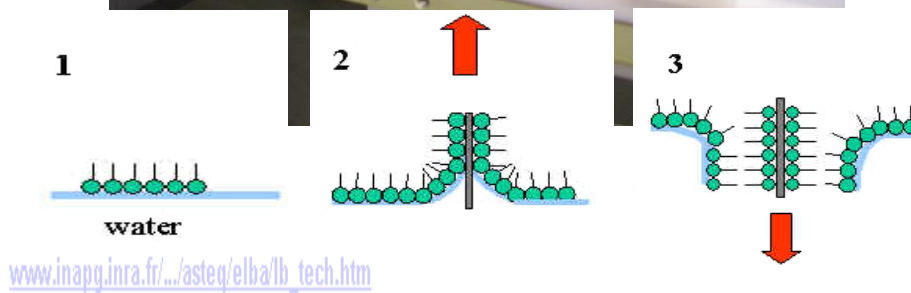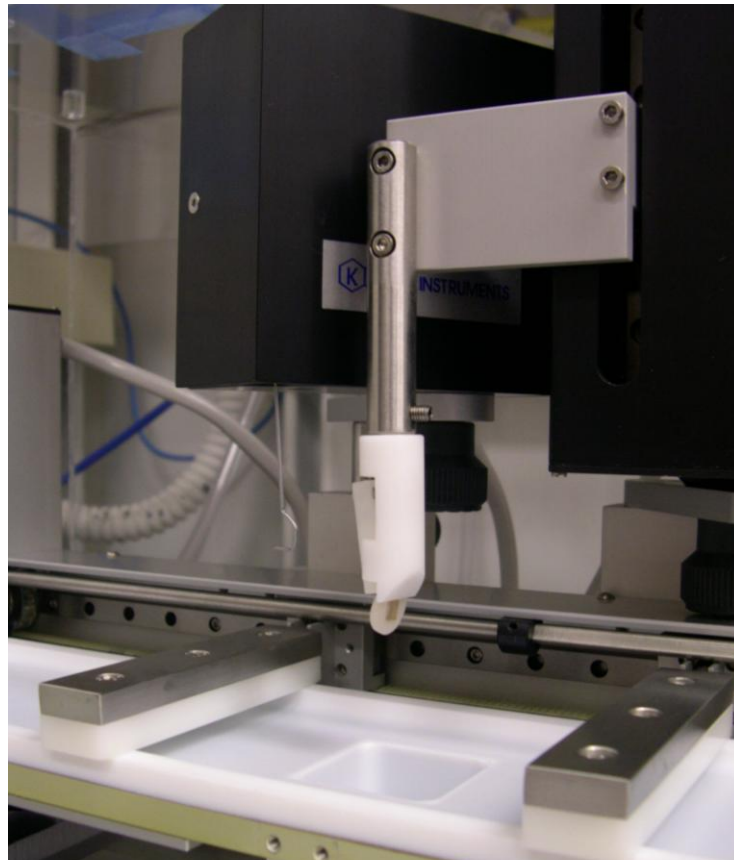
Figure 2. Photograph shows the LB-trough precision deposition arm loaded with a mica substrate bound to its hydrophobic PTFE backing. The cartoon depicts the deposition of a lipid bilayer on to the substrate. **1.** Shows the lipid monolayer with the polar heads touching the water and the lipid tails normal to the water/buffer surface. **2.** After passing the substrate up through the monolayer once, a single lipid monolayer is deposited onto each side of the mica sheet. **3.** The second and final pass back down through the monolayer and into the subphase deposits the second leaflet of the bilayer on each side. This second leaflet can be made of a different lipid than the first, simply by changing the LB monolayer after the first pass.

than that normally achieved by the vesicle fusion method, however intolerably large mica patches again remained exposed (Figure 3).

In a third attempt at achieving high coverage supported lipid bilayers, the mica was treated with poly-L-lysine before depositing the vesicle solution on top of the mica. Simply, the poly-L-lysine solution was placed on the freshly cleaved mica, and allowed to incubate at room temperature for approximately ten minutes. It was then removed by flushing several times with the vesicle fusion buffer as described previously. Poly-L-lysine was used to establish a positive surface charge in hopes of not attracting the BoNT/A protein to the treated surface, as the untreated negatively charged mica surface did. In this manner, near perfect lipid coverage would not be required to prevent the drastic binding of the toxin to the mica exposed in between the lipid bilayer islands. However, this rough poly-L-lysine pre-treatment method resulted in very poor lipid coverage when employed with the vesicle fusion method (Figure 4).

Therefore results reported here depend primarily on the recent technique of employing lipid monolayers formed on Langmuir-Blodgett troughs as model cell membranes.

Langmuir Blodgettry

As an alternate approach and in collaboration with Jarek Majewski and Chad Miller of Los Alamos National Laboratory (Los Alamos, NM) we have been using a lipid monolayer on a Langmuir-Blodgett (LB) Trough (KSV Instruments Minitrough, Finland) as an artificial membrane that allows toxin insertion studies. The LB-trough serves as a controllable, accessible synaptic cleft model. The trough holds a liquid subphase that

13
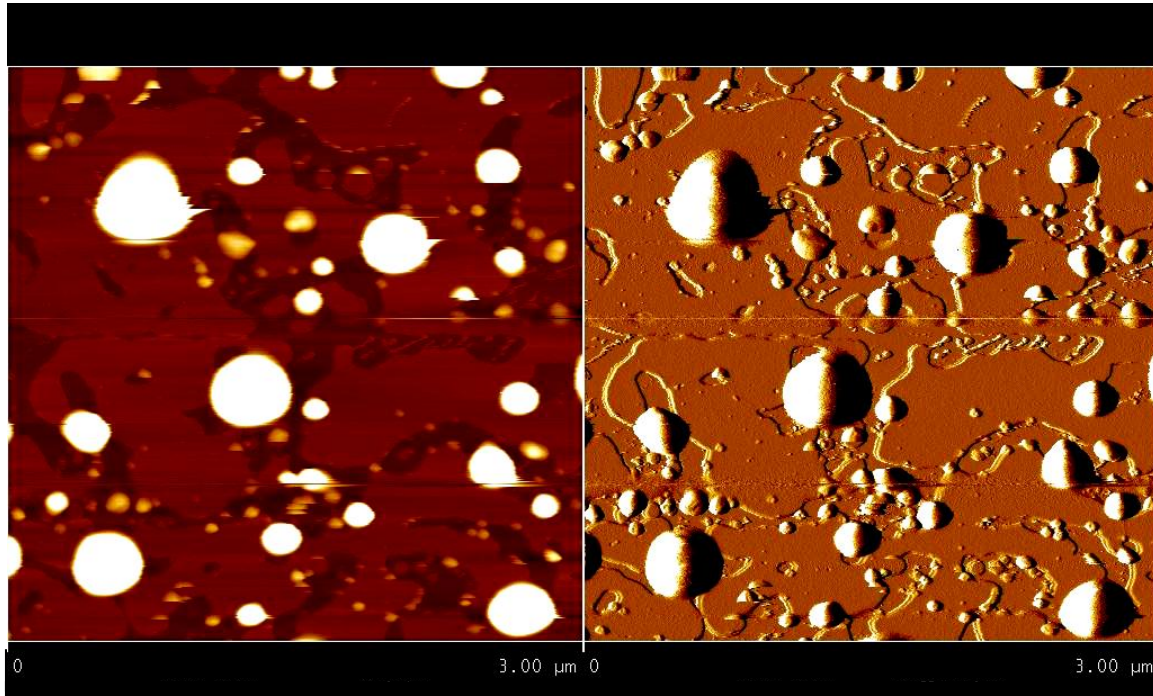
Figure 3. 3μm x 3μm AFM image of an LB-trough-deposited lipid bilayer. The lowest region (as indicated in the darkest color of the height image (left)) is exposed mica. The highest regions, in white are vesicles adsorbed to the bilayer surface. The midgrade brown color reveals an adsorbed lipid bilayer. The edges of these three levels can be more clearly distinguished in the deflection image (right). The LB-Trough lipid bilayer deposition allowed for thorough coverage, but the exposed mica surface, all though less than the typical vesicle fusion method, was still too extensive for the purposes of BoNT/A binding, insertion studies.

14

Figure 4. 8μm x 8μm image of poly-L-lysine pretreated mica was used as the substrate for vesicle fusion lipid deposition. The treatment of the mica appeared to have a stark negative effect on the deposition of lipid via this method.

represents the extracellular fluid in the cleft of the neuromuscular junction. At the interface between this liquid and the air, a mono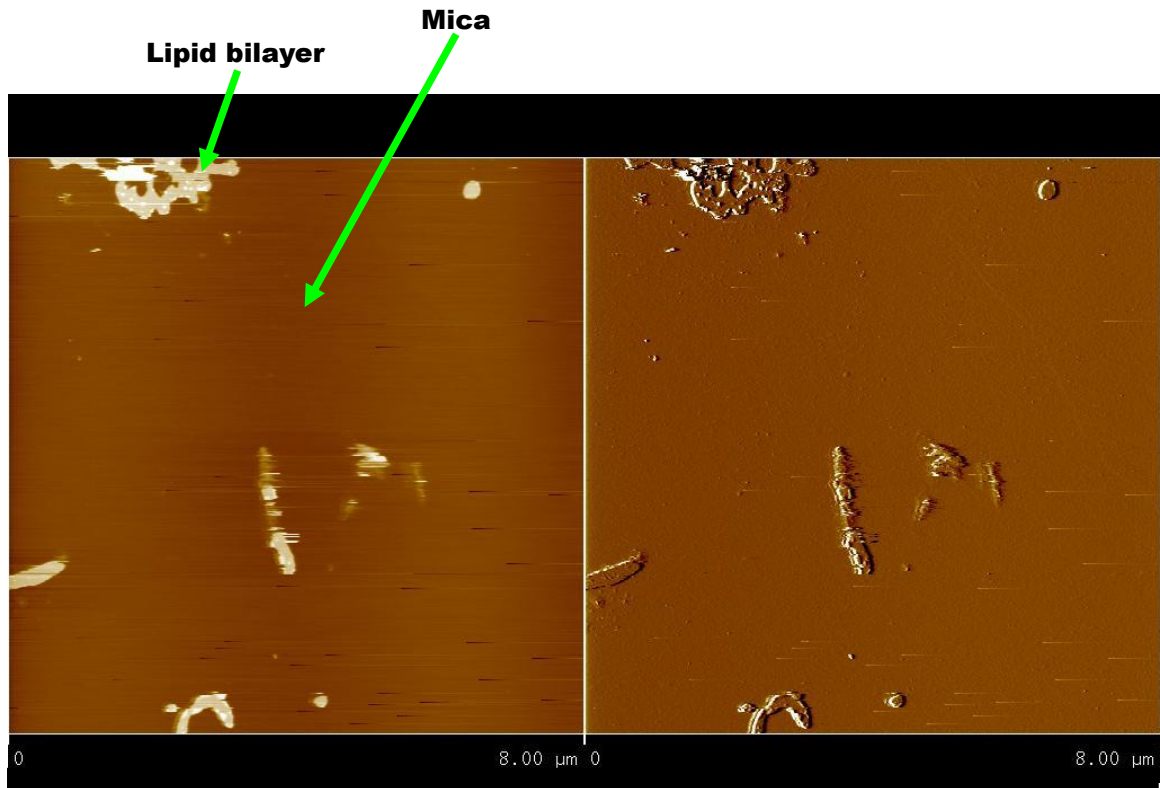layer of amphiphilic lipids is formed. This monolayer models the outer leaflet of the nerve endplate membrane. The monolayer will also represent the inner leaflet of the endosome upon receptor mediated endocytosis. Although only half the membrane is represented by the monolayer system, the membrane's hydrophobic portion of its second half is electrostatically similar to the air above the monolayer. The outerleaflet lipid headgroups and the water above them are missing from our model which must be taken into account for interpretation.

We assumed that the surface pressure on the membrane would have a negligible change due to toxin insertion, given the large membrane surface area to toxin ratio. To mimic this characteristic, we held the monolayer's surface pressure constant. This is accomplished through the negative feedback loop response feature of our KSV Instruments LB-trough. As a membrane associating protein inserts, the surface pressure begins to increase, but is quickly relieved by a corresponding change in monolayer area. This keeps the surface pressure constant (+/- 1 mN/m from the set point value, with a strong mean at the set point surface pressure) (Figure 5) throughout the experiment. Thus, the percentage of monolayer expansion versus time is the measure used to assess the degree of toxin insertion to the membrane. The KSV Langmuir-Blodgett Minitrough's surface pressure sensor is acutely sensitive to changes in level. The use of a vibration dampening air table for the LB-trough ended up producing tilt related fluctuations in surface pressure, which ultimately required us to run calibration experiments that corrected for changes in level on surface pressure readings.

Due to the high cost of our toxin samples, an ultra small volume custom LB-

trough was constructed. We designed the LB-trough to not only hold a small volume, but also be compatible with the remainder of our commercial KSV Instruments LB Minitrough. The custom LB-trough was made out of milled PTFE stock. The final dimensions were 65.1mm x 18.28mm x 3.25mm. Our custom LB-trough walls had thicknesses of approximately 1mm. After milling, the final custom trough's surface roughness was achieved with wet one-thousand-grit sand paper. When the custom LB-trough was filled with buffer to a typical initial level, which always had a positive meniscus, it held approximately 4.7ml (Figure 6). This is in contrast to the commercial LB-trough which holds approximately 83ml, once the deposition well is covered.

Paper Wilhelmy plates (PWP) were used with the surface pressure sensor. The PWPs were cut from Whatman filter paper. PWPs were calibrated before each run against the standard of pure water surface pressure or a standard weight. Eventually the PWP was replaced with a microroughened platinum Wilhelmy Rod (PWR) (KSV Instruments, Finland) when our surface pressures were held above 20mN/m, as the PWP was no longer reliable in that range (20).

Cleaning of all contact surfaces of the LB-trough was performed with a 2% sodium octanoate detergent solution (octanoic acid, sodium salt, 99%, Aldrich Chemical Company, Inc. Milwaukee, WI), then with a fresh, high-purity grade chloroform (stabilized with a non-polar hydrocarbon) (Omnisolv). The LB-trough barrier was made of Delrin and was rinsed with acetone, (because Delrin is solubilized by chloroform). The LB-trough and barrier were then immediately rinsed in ultra pure water (Nanopure Milli-Q filtering system) in order to minimize any trace amounts of non-volatile particles the solvents would have otherwise left behind. In most cases the LB-trough was then
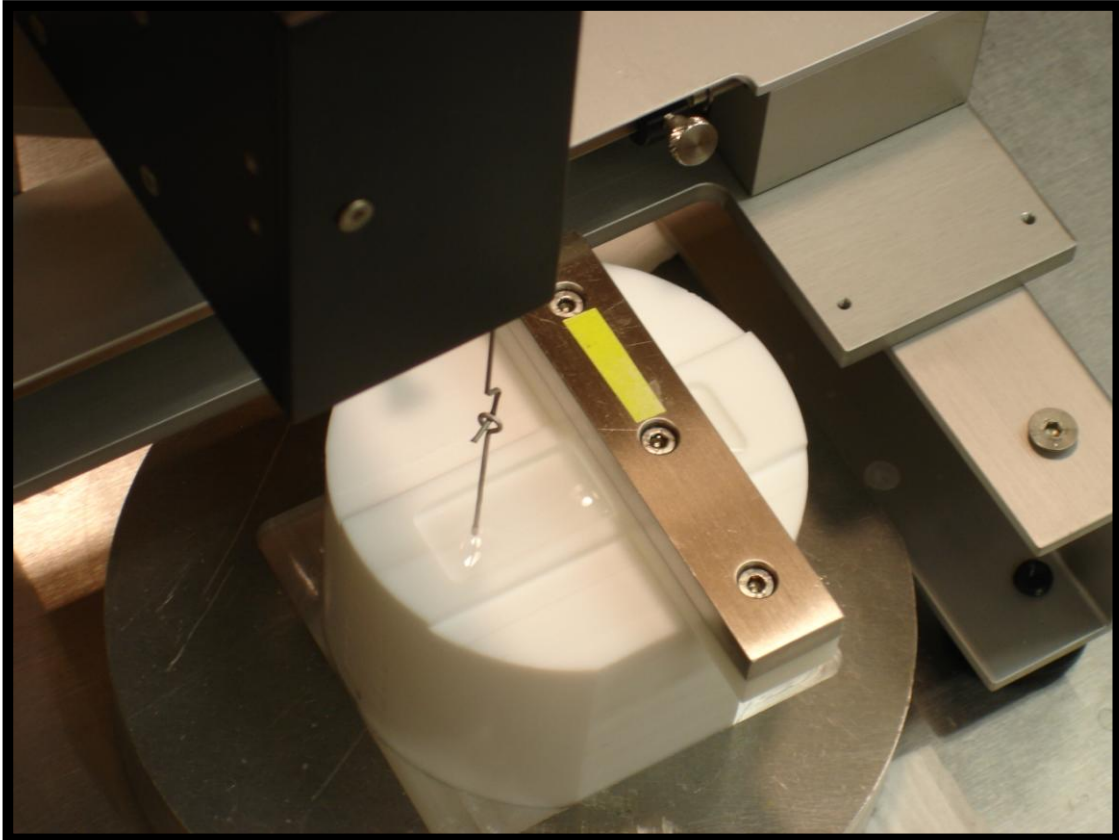
Figure 6. This photograph shows our custom LB-trough. Its dimensions are 65.1mm x 18.28mm x 3.25mm. With a typical initial positive meniscus, the custom trough holds approximately 4.7ml.

filled with a freshly prepared pH 4.8 or pH 7.4 phosphate citrate buffer (Sodium Phosphate, dibasic. Fisher, Lot No. 897108; Citric Acid, Monohydrate. Fisher, Lot No. 922504). Laboratory quality sodium chloride was then added to bring the ionic strength of the buffer up to the desired level.

- The pH 4.8 buffer used for all monolayer experiments held at 20 (+/- 5) mN/m had 239.2mM Na^+, 140mM Cl^-, 49.6mM $H_2PO_4^-$, 25.2mM $HC_3H_7O(COO)_3^{2-}$, resulting in an ionic strength of 243mM.

- The pH 7.5 buffer used for all experiments held at 20 (+/- 5) mN/m had 314.4mM Na^+, 140mM Cl^-, 87.2mM HPO_4^{2-}, 6.5mM $C_3H_5O(COO)_3^{3-}$, resulting in an ionic strength of 430.9mM.

- The pH 4.8 buffer used for all experiments held at 30 (+/- 1) mN/m had 158.4mM Na^+, 118.4mM Cl^-, 20.0mM $H_2PO_4^-$, 10.3mM $HC_3H_7O(COO)_3^{2-}$, resulting in an ionic strength of 160mM.

- The pH 7.7 buffer used for all experiments held at 30 (+/- 1) mN/m had 119.3mM Na^+, 63.5mM Cl^-, 111.6mM HPO_4^{2-}, 12.1mM $C_3H_5O(COO)_3^{3-}$, resulting in an ionic strength of 153mM.

Phosphate-citrate was chosen due to its large variety of pKa's. This allowed us to buffer well at both of the pH values we were interested in, without altering the salt species.

Before lipid deposition, it is necessary to rid the subphase air-water interface from trace amounts of surface active molecules, which contribute to the surface pressure. This was accomplished by translation of the Delrin LB barrier to one end of the trough. The barrier slowly skims along the subphase surface, pushing in front any surface active

molecules that may be present. If there are surface active molecules, an aspiration pump

fixed with a thin gel electrophoresis loading pipette tip was manually tapped along the

subphase surface, removing any contaminants. The LB barrier was then translated back

down the trough. If the surface pressure sensor did not change from its arbitrary initial

value after compression, the air-water interface was considered clean and the surface

pressure was then defined to be zero. This calibration is in accordance with the standard

of pure water, which is defined to have a surface pressure of zero. Cleaning and

calibration was done before every experiment.

The lipid monolayer was made of DPPC or 1,2-dipalmitoylphosphatidyl-

glycerol (DPPG) (Avanti Polar Lipids), mixed with 20% GT1b (Sigma Aldrich) or Total

Ganglioside Extract (porcine brain, ammonium salt. Avanti Polar Lipids. Lot #TGANG-

14) by mole fraction. This lipid mixture was suspended in a volatile solution not miscible

with water. Many lipids including DPPC and DPPG are very soluble in the volatile

solvent Chloroform, which is not miscible with water. However, gangliosides have a low

solubility in chloroform. The gangliosides were first solubilized in a minimal amount

(1.5% by total volume) of high purity methanol (Mallinckrodt Nanograde). Once they

were dissolved in the methanol they could be added to the lipid-containing chloroform

without falling out of solution.

This solution is placed drop wise using a glass, gas-tight syringe (Hamilton,

Reno, NV) onto the air/water interface of the LB subphase, such that the solution quickly

diffuses over the surface as its volatile solvent evaporates, leaving behind the amphiphilic

lipid and charged gangliosides. This forms a lipid monolayer on the subphase surface

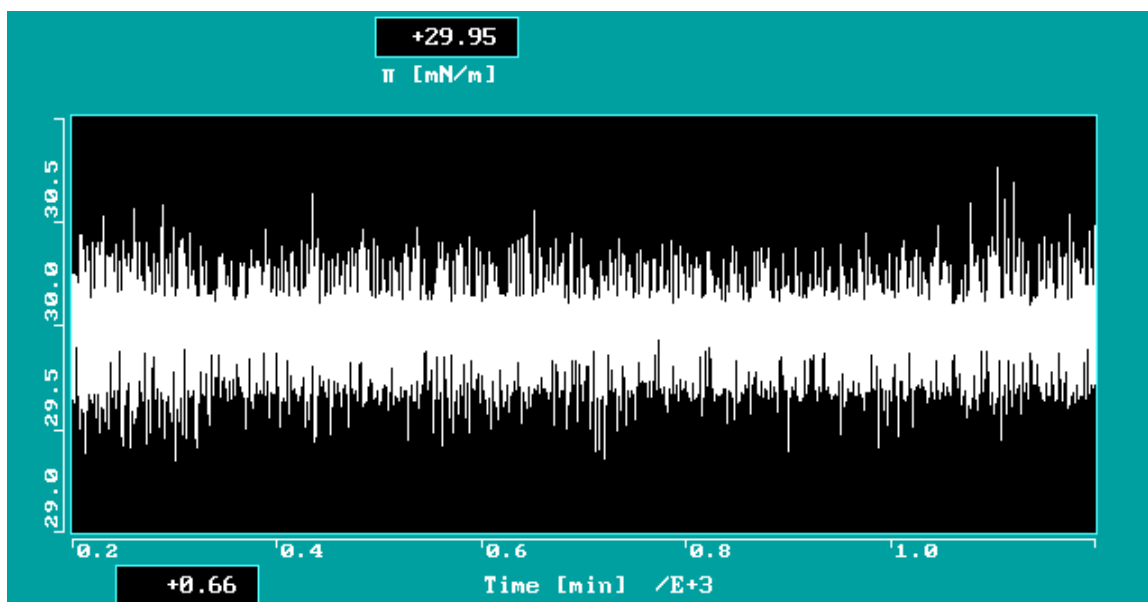with the lipid heads down to the water and the lipid tails up in the air. The gangliosides

Figure 5. Representational graph of typical surface pressure readings. The mean surface pressure holds tightly around its set point value even as the monolayer makeup changes due to BoNT/A insertion. The y-axis is surface pressure in mN/m, and the x-axis is time in minutes x 10^3.

are dispersed throughout the lipid molecules.   As the LB barrier compresses the monolayer it becomes highly ordered , like that of the inner leaflet of a membrane. We compressed our monolayer until the surface pressure reached 20 (+/- 5) mN/m.

Once a baseline was obtained to check for drift, BoNT/A heavy chain, heavy chain quarter (HCQ) which is the C-half of the C terminus of the heavy chain (27), or the detoxified form of the holotoxin was added. All of these BoNT/A proteins were kindly donated by Dr. Bal Ram Singh of the University of Massachusetts, Dartmouth. The detoxified recombinant form of BoNT/A (DR BoNT/A) has been altered with neutralizing mutations at two specific sites, E224-to-glutamine and E262-to-alanine, within the active site of the light chain. According to ELISA activity assays (19), these mutations eliminate light chain endopeptidase activities against the light chain substrate SNAP 25. Additionally, bioassays were performed to study the effects of DR BoNT/A. Groups of mice were injected with increasing doses of DR BoNT/A, their survival was monitored. Mice receiving doses of DR BoNT/A as high as 0.0625 µg/g (131,000 times the minimum lethal dose) demonstrated no symptoms of botulism. This indicates that DR BoNT/A has a toxicity 100,000-times lower than native BoNT/A. Further, DR BoNT/A was used to immunize mice, which provided complete protection against native BoNT/A, showing that DR BoNT/A structure is similar to the native toxin because antibodies raised against DR BoNT/A recognized both the mutated and active holotoxin. Through far-UV circular dichroism spectroscopy, it has also been determined that the secondary structure of DR BoNT/A is essentially visually identical to that of the native neurotoxin (personal communication Bal Ram Singh).

The toxin was added to the subphase of the LB-trough by penetrating the

monolayer with the needle of a Hamilton microsyringe. The typical volume of toxin

solution injected was around 175μl, which resulted in an increase in surface pressure

reading. However the the syringe needle itself appeared to drop the surface pressure by

removing a small amount of the lipid molecules upon retraction. The net effect of these

two alterations was a mild drop in surface pressure reading that resulted in a small area

compression. This was done to yield a final toxin concentration of approximately 0.2μM.

     To minimize microscopic monolayer perturbations, the LB-trough was placed on

a laboratory vibration dampening air table, although side effects were problematic, as

stated above. The shallow depth of the custom trough (3.25mm) also helped to minimize

the height of waves in the subphase surface. Further, no external pumps, nor stir bars

were used to speed up toxin diffusion in order to keep the monolayer as undisturbed as

possible. Stir bars and pumps caused visual disturbances in the monolayer, even when

the 0.5mm thick stir bar or the peristaltic pump were turned on to their lowest settings.

Instead the injection was done through several places in the lipid monolayer to maximize

the mixing of the toxin into the subphase. The chamber was then left alone to mix by

diffusion. Experiments with food coloring showed that this injection method mixed

thoroughly below the monolayer in approximately 15 minutes. Complete diffusion

throughout the custom LB-trough took nearly 150 minutes.

     It was found that azolectin monolayers made from soy lipids were not ideal

because of their unstable surface pressures, given a fixed area. Wide LB-trough walls did

not allow for stable monolayers consistently. In order for the Delrin LB barrier to ride

true against the custom LB-trough walls, it was necessary for the walls to be narrow,

about 1mm wide (Figure 6).

RESULTS

ATOMIC FORCE MICROSCOPY

When toxin-incorporated vesicles were used, the AFM revealed that the vesicle fusion method worked significantly less effectively than it did with pure lipid vesicles. Measures were taken to compensate for this by sonicating longer, sonicating in warm water, and incubating the sample over the mica longer. The result was more lipid on the mica surface, however it was in excess. The mica was usually found completely covered with a single lipid bilayer, with additional lipid micro domains on top. In order to see the primary bilayer the AFM tip was used to purposely scan with an excessively high pressure and tip velocity to remove the extra lipid. This would consistently leave only the bottom lipid bilayer with near perfect coverage (Figure 7). On many occasions, promising distinctions arose between images of pure supported planar DPPC bilayer controls and samples with the addition of BoNT/A heavy chain (Figure 8). 14, 1-μm^2 control images, and 7, 1-μm^2 BoNT/A heavy chain images were searched, and raised elements counted. Sample results are reported in Table 1. The search criterion was three-fold. Typical amplitude images exhibit interference of a couple angstroms. The minimum element height was therefore set at 4 angstroms. The maximum was 5 nanometers – chosen because small lipid layers are often as small as 5.5 nanometers. Elements were grouped by height. A correction was made for the area of fused bi-layer in the sample. For example, if an image was found to be 73.28% fused bi-layer by area, the element-per-square-micron figure was obtained by dividing the number of observed elements by 0.7328. The final row of Table 1 contains the probability that the difference
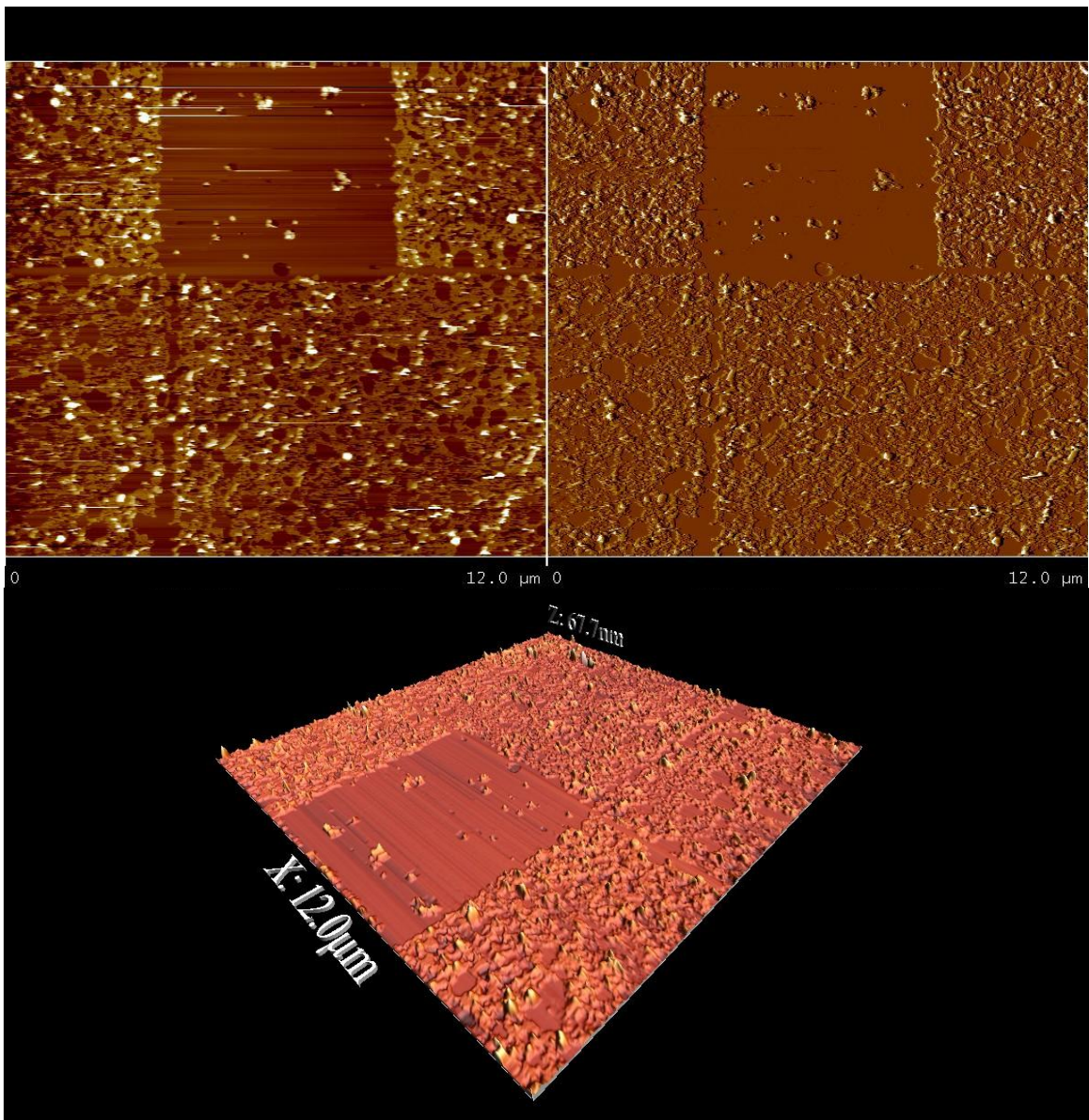
Figure 7. AFM image of excess lipid being removed revealing one lipid bilayer. All three images are different renditions of the same topography of a pure DPPC sample on mica in pH7.4 sodium phosphate buffer. The top left scan is the "height" image, which is produced by the AFM piezoelectric movement. This scan has a z "grey scale" of 33.5 nanometers, where black is zero and white is 33.5 nm or larger. The top right scan is the deflection image of the same topography, which is produced by the AFM cantilever movement, or "deflection." All three renditions show, after zooming out, the square section of removed lipid by the AFM tip's high pressure/fast scanning. Bottom is a 3-demensional rendition of the hieight image. The total scan size is 12μm x 12μm. 3-demensional image created with WSxM v3.0 Beta 11.4 software, available through Nanotec Electronica S. L.
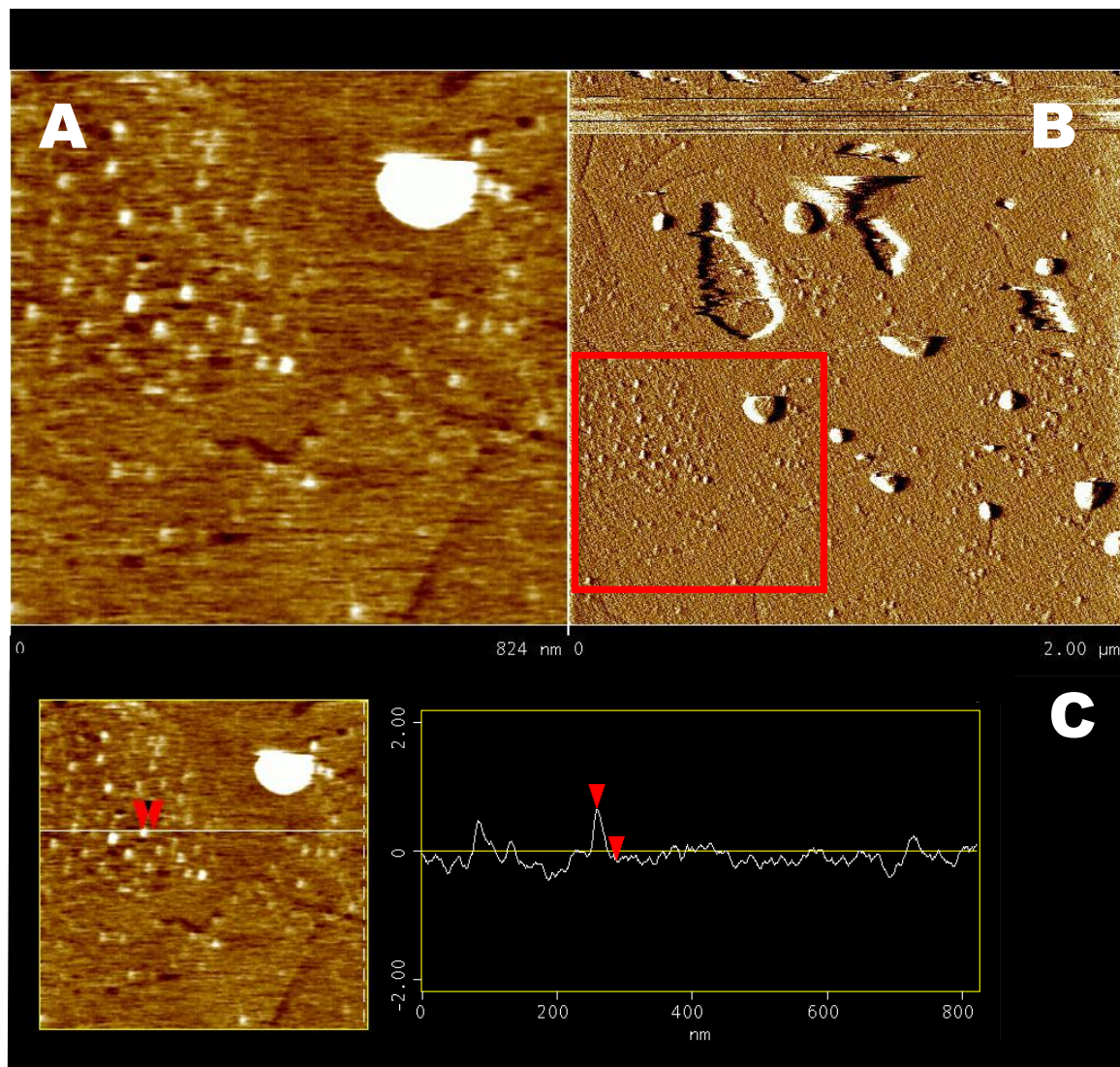
Figure 8. A 0.824μm x 0.824μm height AFM image of the suspected BoNT/A Heavy chain, inserted into a DPPC supported bilayer. **B** 2μm x 2μm AFM image depicting the deflection of a DPPC supported on mica bilayer that had been incubated for 28 minutes with BoNT/A Heavy chain. The red box describes where the zoomed in box B hight image came from. **C** A cross section of box B. The cross section location is indicated on the left, and its actual cross section is on the right. The height of the suspected BoNT/A Heavy chain is measured as 0.8 nm.

26

Element size (nm)	[0.4,0.6)	[0.6,1.0)	[1.0,2.0)	[2.0,3.0)	[3.0,4.0)	[4.0,5.0)
x (protein)	5.50	11.64	10.51	0.63	0.29	0
μ (control)	2.68	3.98	2.61	1.37	0.12	0.56
x-μ	2.82	7.66	7.90	-0.74	0.18	-0.56
σ	3.41	3.34	1.96	1.69	0.44	0.98
(x-μ)/σ	0.83	2.29	4.04	-0.44	0.41	-0.58
$P(\sim H_0)$	71.96%	98.90%	≈100%	N/A	65.89%	N/A

Table 1. The average number of particles per μm^2 of bilayer x, is reported for the size range listed in the header for each column. 1mg DPPC / 10mg BoNT/A heavy chain / 0.1 ml was the original subphase concentration the 250μl droplet. The excess was rinsed away. The mean in protein free control samples is given in the second row as μ (control). The difference, standard deviation for x, and ratio are used to compare $P(\sim H_0)$. The probability that the null hypothesis is false (i.e. that there are more particles in the test case than control) from a single tailed T test is listed in the bottom row.

between protein sample mean and control mean did *not* arise by random chance. Most significant are the differences found in elements of height between 0.6 and 2.0 nanometers. This points strongly to these elements as candidates for BoNT/A heavy chain proteins.

When we diluted the toxin incorporated vesicle solution from 1mg/10mg/0.1ml (lipid/BoNT/A Heavy Chain / Solution volume) to 1mg/10mg/1.0ml we found that through the vesicle fusion method it was easier to achieve good lipid single bilayer coverage without excess. When these images were analyzed, significantly fewer topographical particles were counted as compared to the images taken of undiluted sample.

Upon close inspection it was noted that when the fast scanning, high pressure AFM scan was used to remove excess lipid above the primary lipid bilayer, small lipid topological particles (1 to 3 nanometers tall) were agitated loose and adhered to the bilayer, giving the appearance of toxin particles, in the absence of toxin (Figure 9). Therefore, we dismissed the results in Table 1 as likely artifact and abandoned (for purposes of this thesis) the AFM line of experiments.
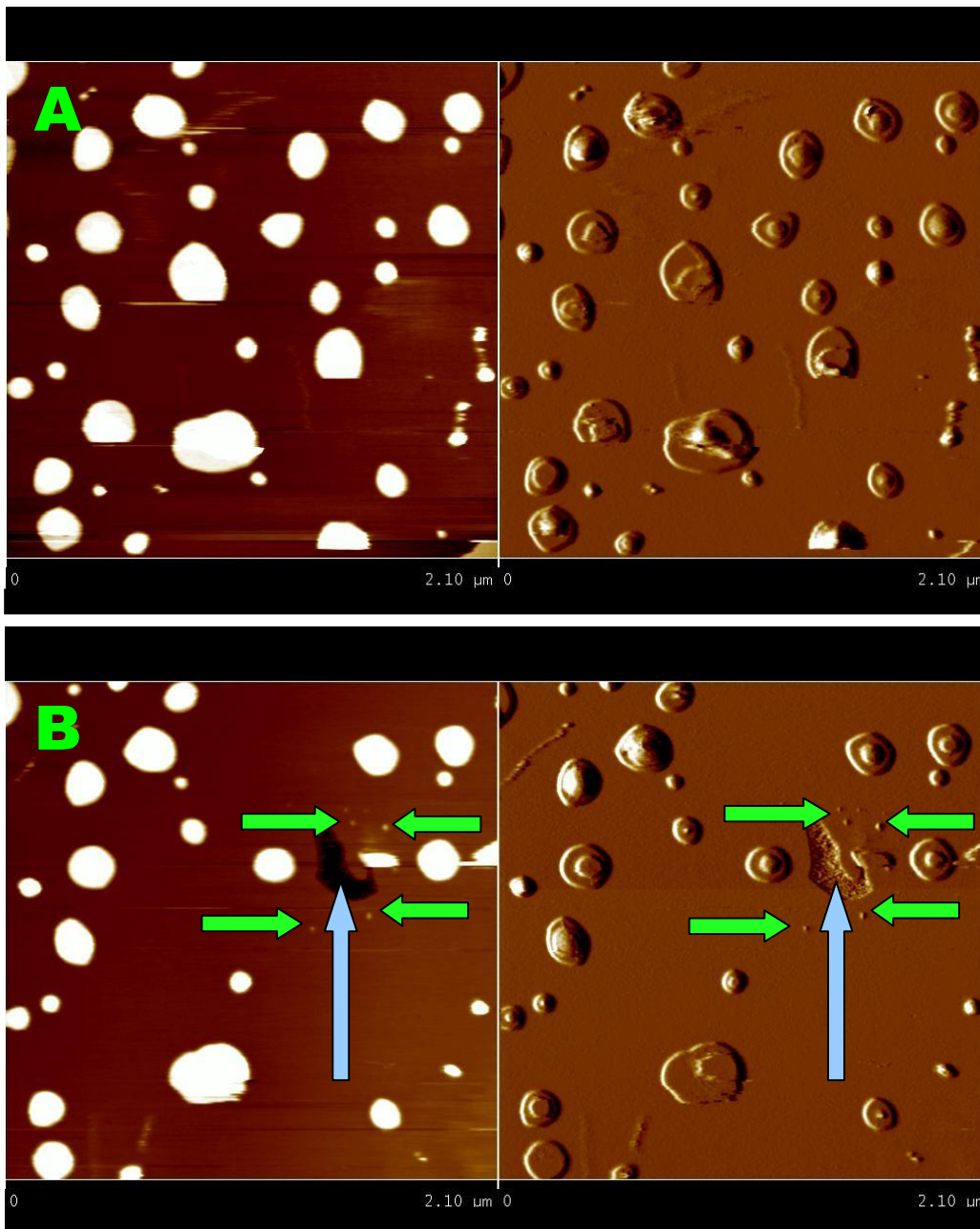
Figure 9. Demonstration that the AFM tip can produce small lipid particles (<1 to 3nm tall). Figure 9-A shows a 2.1μm x 2.1μm scan of pure DPPC. Figure 9-B shows the same sample, in the same location after a high pressure/fast small scan in the upper right hand quadrant. This produced a defect in the bilayer (blue arrow), and small particles (green arrows) of the order seen during past experiments in the presence of unnicked DR BoNT/A.

Langmuir Blodgettry

      The Langmuir-Blodgett custom 4.7ml PTFE trough demonstrated steady, reproducible DPPC/Ganglioside (80:20) monolayer surface pressures after monolayer compression to a fixed area.

      When the surface pressure was held constant at about 20(+/- 5) mN/m or higher, regardless of pH, ionic strength and buffering species in the subphase, a clear expansion of the monolayer resulted after toxin injection. (Figure 10A). In Table 2 of the appendix, a list of all LB monolayer experiments done with 0.1 - 0.2µM BoNT/A are presented. Experiments 1-8 are BoNT/A injections at low surface pressure and 10-15 are BoNT/A injections at cell membrane-like surface pressure. They nearly all show a clear expansion ($\geq$ 10%) of the monolayer. The monolayers were all made of DPPC and GT1b or a mixture of gangliosides at 80:20 by mole fraction. In contrast, the controls (experiments 9, and 16 – 21) show little to no expansion of the monolayer. Conditions for experiment 9 were like those in experiments 1-8, but the DR BoNT/A sample was boiled for approximately 12 minutes. The solution showed obvious DR BoNT/A denaturation as manifest by the appearance of large white aggregates in the solution after heat exposure. Injection of this sample with precipitate suspended gave a diminished monolayer expansion about five-fold below the average. Experiments 17 – 22 are three different controls. Experiments 17 and 18 have no ganglioside receptors in their DPPC monolayer. Under these conditions no monolayer expansion was observed after DR BoNT/A injection. (Figure 10B). Experiments 19 and 20 use the HCQ protein which is BoNT/A heavy chain without the translocation domain (25). HCQ had a negligible monolayer expansion of approximately 3%. Finally experiments 21 and 22 are with the control
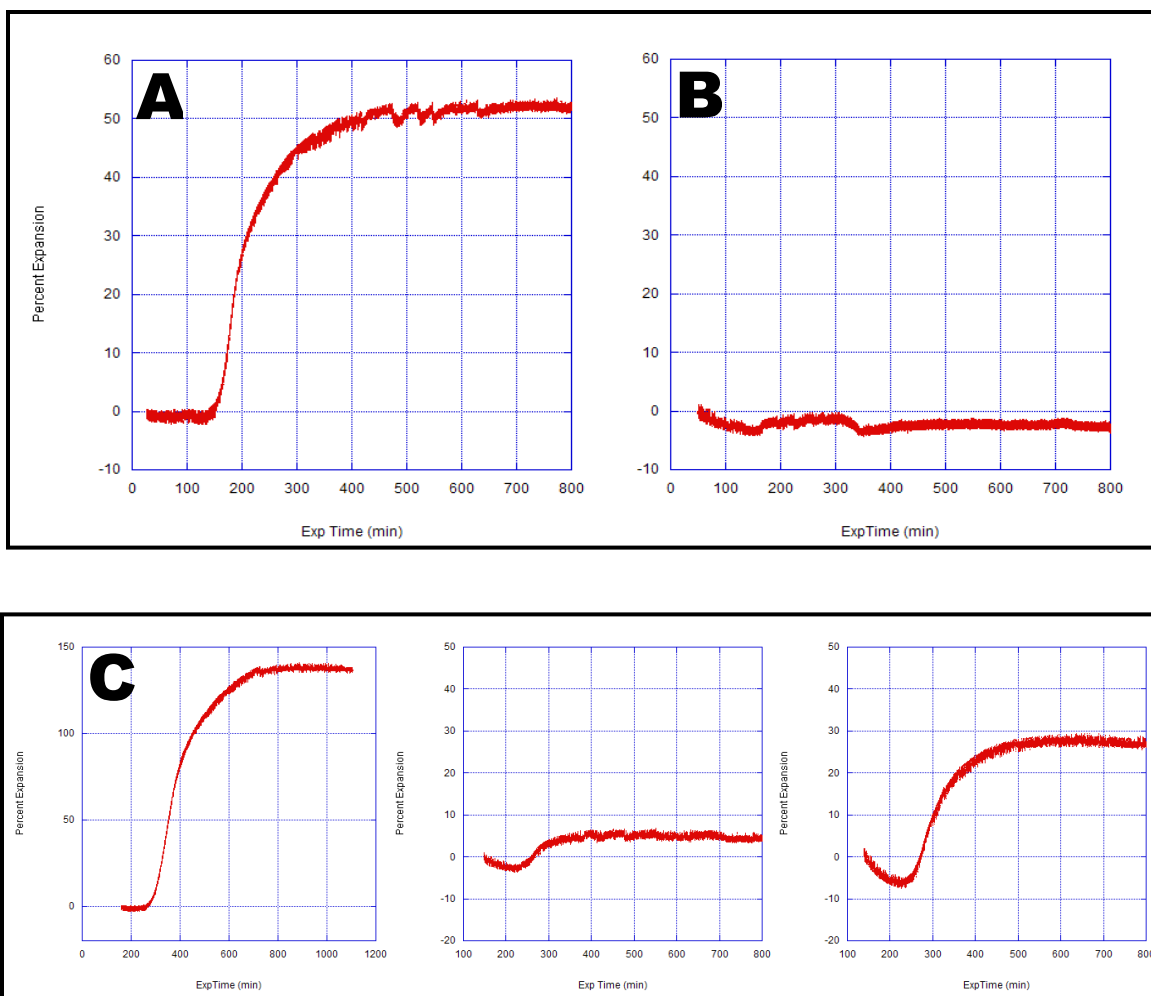
Figure 10. A) DPPC/GT1b monolayer percent expansion (relative to initial area immediately after injection) vs. experimental run time (minutes) due to DR BoNT/A insertion. The tracing starts at the time of toxin injection into the subphase of the LB-trough through the DPPC/GT1b or mixed ganglioside (80:20) monolayer. After a lag time that averaged about 100 minutes the toxin began to insert into the monolayer causing the monolayer to expand under a constant surface pressure. **B)** DPPC monolayer (without ganglioside receptor) percent expansion vs. experimental run time (minutes) after 0.2 µM DR BoNT/A injection. This graph is representative of the negative results acquired by control experiments that consisted of receptor free monolayers, HCQ and Albumin. **C)** Representational graphs demonstrating that the experiments were run long enough to see a steady state. The conditions associated with the graphs found in box C, are located in Table 2 of the appendix. From left to right the file names are: 080207.#00, 082907.#00, and 081007.#00.

plasma protein albumin. Albumin was tested at the standard 0.2 μM and also with a fifty

fold concentration increase at 10.0 μM. DPPC/Total ganglioside extract monolayers

revealed no monolayer expansion at either concentration with albumin (Figure 11).

When the ganglioside concentration is reduced from 20% to 10%, the expansion of the

monolayer in the presence of DR BoNT/A is reduced (Chad Miller and David Busath,

personal communication). In the absence of any gangliosides toxin-induced expansion is

eliminated. When the lipid monolayer is switched from the zwitterionic DPPC to the

negatively charged DPPG (identical ions in the bath, both lipids containing GT1b, and

the toxin concentration remaining at 0.2μM), DR BoNT/A inserts into the monolayer

more readily (tested at low pH only).

Figure 12 is a bar plot that summarizes the data of Table 2 by grouping the

experiments into relevant categories. The categories focus on BoNT/A version, and

subphase pH. Figure 12 must be recognized as preliminary results. These data have

shaped are hypothesis and will guide are future emphases, however more work is

required before this data can be considered compelling. Comparing groups within Figure

12, one to another through formal statistical methods is largely inappropriate. The N

values of each group are not large enough to possibly form normal data distribution

curves. The standard deviation, to which so many statistical tools are connected, is based

on the mean of the data. The mean of the data only represents center accurately when the

data distribution is normal. Unfortunately, these variations between experiments are too

large to allow analysis of how environmental variables (pH, ionic strength, surface

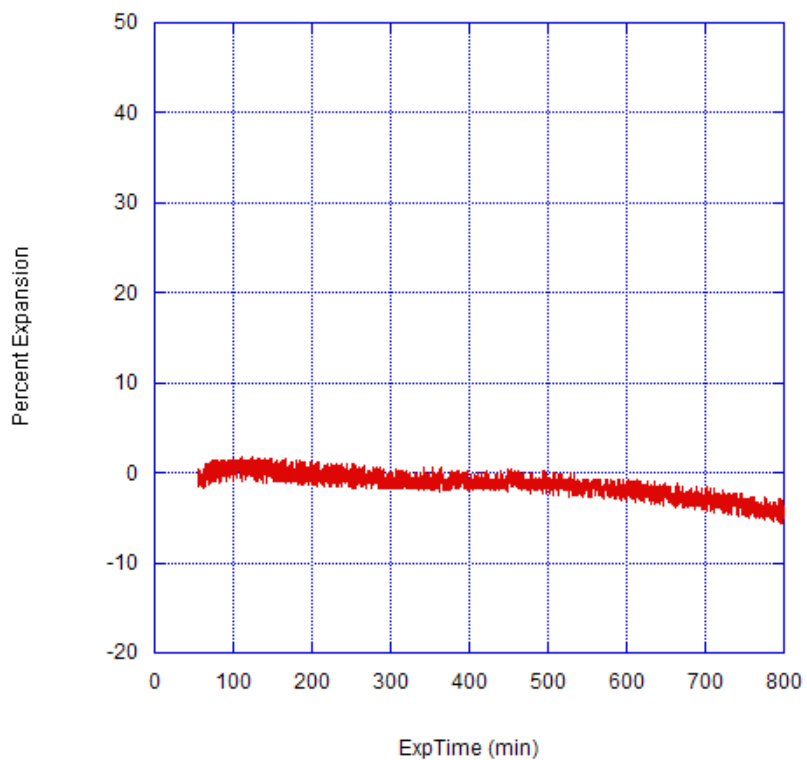pressure, and temperature) affect the final percent expansion.

Figure 11. LB expansion graph of the control protein Albumin. The eventual area compression is due to slow evaporation from the LB-Trough. With this understanding it is clear that expansion due to Albumin is negligible. This was done with a phosphate citrate buffer at pH 4.8, and an ionic strength of 160mM.
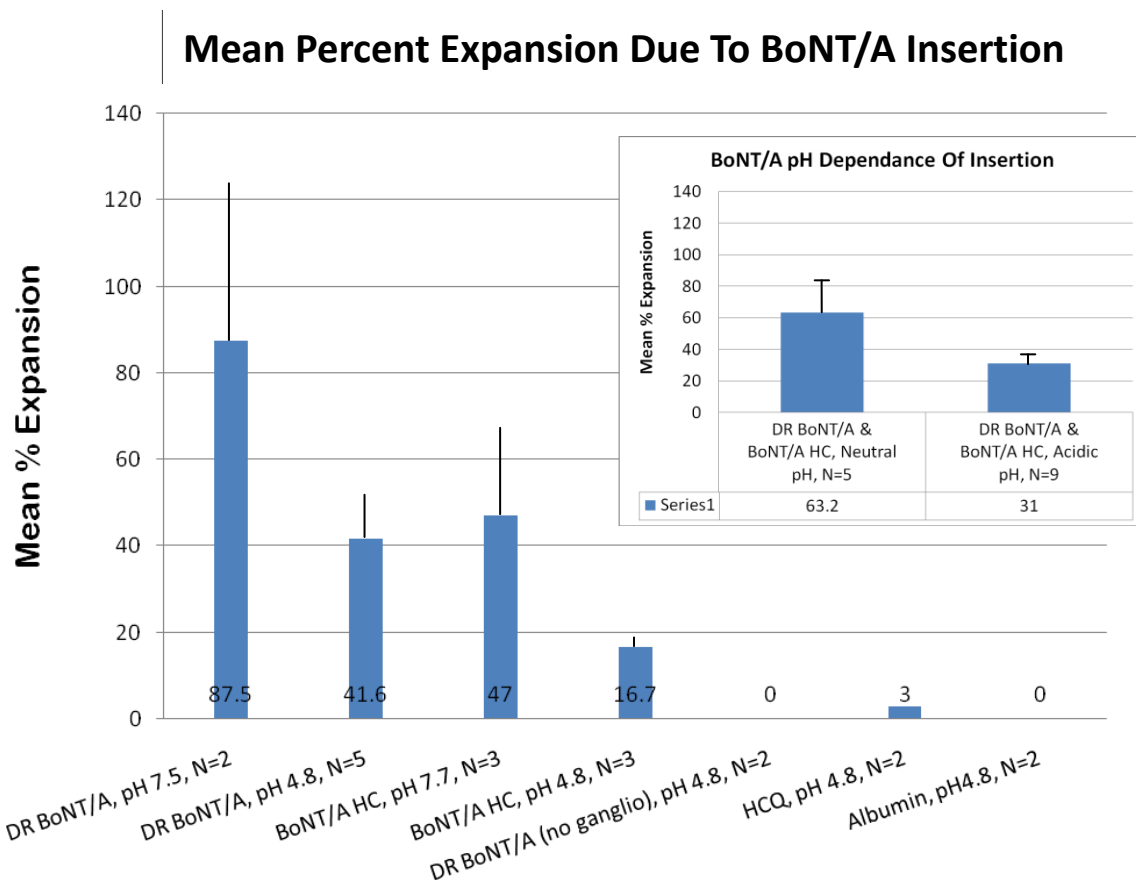
Figure 12. Bar plot of various experimental groupings with essential parameters listed under each. The details of each experiment and their variations within groupings are contained in Table 2 of the appendix. The line above each bar represents one half of the standard deviation. When combining the first four bars into one "insertable" group, a mean of 35.1 % expansion with a standard error of the mean (SEM) at 9.4 results. Further, a combination of the last three bars into a "non insertable" group results in a mean percent expansion of 1, and an SEM of 0.6, revealing the two groups as statistically different. The inset bar plot shows only those experiments that include all essential features for monolayer insertion, grouped according to pH. The flag represents one SEM. Neutral pH approaches but does not reach a statistically significant difference over the acidic pH group. Appropriate formal application of statistical analysis will require greater N values. As a whole, there is evidence that gangliosides in the lipid monolayer, and the heavy chain with both translocation and ganglioside binding domains are minimum requirements for toxin insertion into the monolayer in a pH independent manner.

Discussion

Atomic Force Microscopy

The particles created in the control samples that had no toxin present by wiping away the excess lipid with the AFM tip were within the size range of the particles previously assumed to be BoNT/A Heavy chain. An explanation as to why the quantity of so-called toxin particles found decreased when the toxin containing vesicle solution was diluted is simple. The diluted BoNT/A heavy chain vesicle solution was easier to adsorb to the mica. We were able to produce appropriate lipid coverage without the excess. The result was less agitation required by the AFM tip to remove excess lipid. The less this relatively large scale cleaning took place, the less the tiny particle confounders were created. The distinction between toxin particles and tip induced lipid particles proved unresolvable with the AFM and these sample preparations. At this point the decision was made to set this project aside and shift to the recently discovered LB monolayer technique, being used for neutron reflectometry studies by Dr. Busath's collaborators at Los Alamos National Lab for measuring toxin insertion.

In the future, a significant increase in toxin concentration may be used to positively identify the BoNT particles with AFM, on an asymmetric supported bilayer containing gangliosides. Additionally a minimally intrusive tag may also work to positively identify BoNT/A protein in a supported bilayer. Avoiding a tag altogether until after AFM imaging seems least intrusive of all, and an adaptation of an ELISA assay to the imaged sample may perform this task well.

As noted earlier, the DPPC supported bilayer was in the gel phase. Cell

membranes are composed mainly by lipids in the liquid phase at body temperature. It seems expedient therefore that the forthcoming supported bilayers used with the AFM ought to be made up of lipids in the liquid phase. If the mobility of the inserted toxin into a liquid phase bilayer is too great for high resolution AFM images, a lipid such as DPPC could be used such that the temperature is raised to be in the liquid phase ($>41^{o}$ C) during incubation, and finally cooled to room temperature during AFM imaging.

With the advantage of hind sight, this skepticism over the existence of BoNT/A heavy chain in the supported DPPC bilayers is further bolstered by the LB data that shows *no* monolayer expansion by the toxin in the absence of gangliosides, indicating that the toxin does not insert into a pure DPPC membrane. Honing of the LB deposition technique to produce asymmetric bilayers on mica, such that gangliosides and/or other BoNT receptors can be incorporated into the outer leaflet may prove to be the best way to prepare model membranes for future AFM studies.

Langmuir Blodgettry

BoNT/A does not expand a pure DPPC monolayer as our controls show. However, in the presence of gangliosides it does expand the monolayer. This indicates that gangliosides alone can facilitate BoNT/A insertion and potentially BoNT/A light chain exit from the endosome, even in the absence of the high affinity binder SV2.

The DPPC/ganglioside monolayer did not expand with our control protein, albumin. Albumin was chosen because it is an abundant plasma protein that, as such, is considered unlikely to interact with cell membranes. If albumin molecules were to interact by insertion into the monolayer, it would be manifest in monolayer expansion to

36

a similar degree to that of DR BoNT/A or BoNT/A heavy chain. The molecular weights (bovine serum albumin (~66 kDa), DR BoNT/A (~150 kDa) and BoNT/A (~100 kDa)) are close enough to allow us to assume that the degree of monolayer area increase due to insertion by one, is likely to be similar to the others. Even more conservatively we could say that a control protein half the size of the sample protein is very unlikely to insert into the monolayer unnoticed, while the sample insertion is clear. Our results refute the possibility that our monolayer expansions, in the presence of DR BoNT/A, were actually due to features of our monolayer and/or LB setup, independent of the protein makeup.

Our LB percent expansion results extended up to a maximum of 140 percent We found no theoretical basis for disallowing this maximal expansion. Given an approximate initial monolayer of 421 mm^2, at 20% ganglioside by mole fraction, we would have roughly 1.7×10^{14} ganglioside molecules if we assume the area of ganglioside in the monolayer similar to DPPC (48.6 Å^2). At 0.2μM there is more toxin than ganglioside. If each ganglioside were to allow one DR BoNT/A (an approximate sphere of diameter 7.5nm) to bind and insert into the monolayer, the toxin would expand the monolayer ~9,600 mm^2, or 2,300 % expansion. Thus, less than 7% of the toxin inserts.

Figure 12 demonstrates that, in nearly all experiments, BoNT/A expanded the monolayer by 10% or more under conditions where the current BoNT/A hypothesis would predict insertion. Namely, when the ganglioside binding domain and the translocation domain are both a part of the toxin (this would include both the detoxified holotoxin DR BoNT/A and the BoNT/A heavy chain), BoNT inserts into the model membrane, so long as gangliosides are present. We therefore believe that LB monolayers can be considered a promising model for future BoNT/A studies.

37

It is not known when BoNT/A heavy chain inserts into the nerve ending at the neuromuscular junction, nor is the role of acidification understood in BoNT/A heavy chain insertion. The addition to the current popular working hypothesis which is raised by the data of this study, is that insertion of the BoNT/A heavy chain into the membrane does not need to wait until acidification of the endosome, and may even occur before BoNT receptor mediated endocytosis. At both neutral pH (extracellular pH) and acidic pH (late endosome pH), our results show that when the complete heavy chain is exposed to monolayers containing the ganglioside receptor, not just a peripheral binding, but an interaction with the membrane, intimate enough to cause monolayer expansion, occurs. It is our interpretation that this interaction is not a mere binding, therefore, but an insertion. The evidence comes from two results. One, binding without inserting would cause little to no noticeable monolayer expansion, and second, only when the BoNT/A insertion domain is present do we see monolayer expansion.

We extrapolate this data to the native toxin, and believe that the role of acidification in the endosome is not to enable BoNT/A heavy chain insertion into the late endosome membrane, but, rather, it plays the critical role of final conversion of BoNT/A heavy chain into the pore conformation, and/or it prepares the light chain's secondary structure for its translocation.

When more DR BoNT/A and its truncates become available to our laboratory, all of the experiments need to be further reproduced. Several possible confounders have persisted throughout the project, namely:

- unreliable condition of DR BoNT/A and its variants,
- uncertainty in our surface pressure measurements due to air table leveling

inconsistencies, and

- inherent deviations in our model system from nature such as the monolayer itself, unphysiological concentrations of the toxin in the subphase, and an unnaturally large ratio of gangliosides in the monolayer.

The last factor is most acceptable, and even arguably advantageous when looked at with a minimalistic point of view. The monolayer, having air above the lipid tails, necessarily stops the toxin from completely translocating, halting its progress at a stage that might otherwise not have been testable. The high toxin concentrations used allow us to measure readily what otherwise may have been too subtle an effect to notice.

Another major draw back to the monolayer model, is that when the monolayer is made up of more than one type of molecule, the distribution may be erratic. It is possible that, instead of a homogeneous mixture, there segregated domains can form. It is also possible that the extent of this domain formation varies significantly from experiment to experiment, depending on uncontrollable trace contaminants in the monolayer solution or subphase. This unpredictable nature may contribute to the large interexperimental variance we have observed.

The uncertainty in the surface pressure was discovered near the end of the project and was found to be due to the tendency of the vibration table to re-level imprecisely after a weight change to its surface. This was remedied for the high surface pressure (30mN/m) experiments by disabling the air floating mechanism of the table. Calibration tests demonstrated the surface pressure stayed within 1 mN/m of its target with the vibration table disabled, whereas previously our surface pressures were dropped because of table relabeling from the set point value by 5to15 mN/m; and, then the surface pressure

would hold to within 1 mN/m of that dropped value.

The initial experiments, therefore, intended to be run at 30mN/m, were actually run at 20(+/- 5) mN/m. The accepted value for a physiologically relevant surface pressure, in the field of monolayer studies, is 30 to 35mN/m. The expansion observed in the higher pressure strongly suggests that the protein could insert into cell membranes as well.

The final issue of whether the protein might have been partly degraded in some of the experiments is the most difficult to assess. Because the toxin we use has point mutations in the active site of the BoNT/A light chain, it has no enzymatic activity, so enzyme activity assays cannot be used to test the integrity of the protein conformation. Antibody binding assays could be performed but they would only indicate the condition of one small motif, which may or may not pertain to the aspect of the protein of interest. Therefore small, frequently prepared, freshly cloned nicked batches of the mutated toxin should be used in the future, rather than the large infrequent batches we have worked with in the past.

In conclusion, AFM studies of BoNT/A on supported ganglioside-incorporated asymmetrical bilayers indicate potential as significantly contributing tools in this field of toxin research. The LB-trough data demonstrates that this model for toxin studies is promising. This study indicates that BoNT/A heavy chain can insert both at low and neutral pH. We propose therefore that the required acidification step found elsewhere to be necessary for BoNT/A toxicity, does not involve heavy chain membrane insertion.

Heavy chain insertion may occur as early as within the neutral extracellular fluid of the synaptic cleft, immediately following receptor binding.

References

1. **Arnon SS et al**. Botulinum Toxin as a Biological Weapon. *JAMA* 285:1059-1070, 2001.

2. **Simpson LL**. Identification of the Major Steps in Botulinum Toxin Action. *Annu Rev Pharmacol Toxicol* 44:167-193, 2004.

3. **Kortepeter MG and Parker GW**. Potential Biological Weapons Threats. *Emerging Infectious Diseases* 5:523-527, 1999.

4. **Jost WH**. Other indications of botulinum toxin therapy. *European Journal of Neurology* 13:65–69, 2006.

5. **Silberstein S**. Botulinum Neurotoxins: Origins and Basic Mechanisms of Action. *Pain Practice* 4: S19-S26, 2004.

6. **Kozaki S, Kamata Y, Watarai S, Nishiki T, Mochida S**. Ganglioside GT1b as a complementary receptor component for *Clostridium botulinum* neurotoxins. *Microb Pathog* 25:91-99, 1998.

7. **Kitamura M, Takamiya K, Aizawa S, Furukawa K, Furukawa K**. Gangliosides are the binding substances in neural cells for tetanus and botulinum toxins in mice. *Biochim Biophys Acta* 1441:1-3, 1999.

41

8. **Bullens RWM, O'Hanlon GM, Wagner E, Molenaar PC, Furukawa K et al**. Complex gangliosides at the neuromuscular junction are membrane receptors for autoantibodies and botulinum neurotoxin but redundant for normal synaptic function. *J Neurosci* 22:6876-6884, 2002.

9. **Yowler BC, Kensinger RD, Schengrund CL**. Botulinum neurotoxin A activity is dependent upon the presence of specific gangliosides in neuroblastoma cells expressing synaptotagmin I. *J Biol Chem* 227:32815-32819, 2002.

10. *Black JD, Dolly JO.* Interaction of 125-I labeled botulinum neurotoxins with nerve terminals. I. Ultrastructural autoradiographic localization and quantiation of distinct membrane acceptors for types A and B on motor nerves. *J. Cell Biol. 103:521-534, 1986*

11. **Jahn R**. A Neuronal Receptor for Botulinum Toxin. *Science* 312:540-541, 2006.

12. **Dong M, Yeh F, Tepp WH, Dean C, Johnson EA, Janz R, and Chapman ER**. SV2 Is the Protein Receptor for Botulinum Neurotoxin A. *Science* 312: 592-596, 2006.

13. **Koriazova LK and Montal M**. Translocation of botulinum neurotoxin light chain protease through the heavy chain channel. *Nature Structural Biology* 10:13-18, 2002.

14. **Brian AA and McConnell HM**. Allogenic stimulation of cytotoxic T cells by supported planar membranes. *Proc Natl Acad Sci USA* 81:6159–6163, 1984.

15. **Schabert, F., and A. Engel**. Reproducible acquisition of Escherichia coli porin surface topographs by atomic force microscopy. *Biophys J*. 67:2394–2403. 1994.

16. **Leidy, C, Kaasgaard T, Crowe J, Mouritsen O and Jorgensen K.** Ripples and the formation of anisotropic lipid domains: imaging twocomponent supported double bilayers by atomic force microscopy. *Biophys J*. 83:2625–2633. 2002.

17. **Muller DJ, Fotiadis D, Scheuring S, Muller SA, and Engel A.** Electrostatically Balanced Subnanometer Imaging of Biological Specimens by Atomic Force Microscope. *Biophys J*. 76:1101–1111, 1999.

18. **Hughes T, Strongin B, Gao FP, Vijayvergiya V, Busath DD, Davis RC**. AFM visualization of mobile influenza A M2 molecules in planar bilayers. *Biophys J*. 87(1):311-22, 2004.

19. **Sharma SK and Singh BR.** Enhancement of the Endopeptidase Activity of Purified Botulinum Neurotoxins A and E by an Isolated Component of the Native Neurotoxin Associated Proteins. *Biochemistry* 43:4791-4798, 2004.

20. **Bigalke H, Muller H, and Dreyer F.** Botulinum A neurotoxin unlike tetanus

toxin acts via a neuraminidase sensitive structure. *Toxicon* 24:1065-1074, 1986.

21. **Sharma S, Zhou Y, and Singh BR**. Cloning, expression, and purification of C-terminal quarter of the heavy chain of botulinum neurotoxin type A. *Protein Expression and Purification* 45: 288-295, 2006.

	File Name	Surface Pressure (mN/m)	Ionic Strength (mM)	pH	Lipid (80%)	Gang. Type (20%)	Toxin Spec.	[Toxin] (μM)	% exp.	Initial Area (mm²)
1	081007.#00	20 (+/- 5)	167	7.5	DPPC	Mix	DR BoNT/A	0.2	35	386
2	080207.#00	20 (+/- 5)	167	7.5	DPPC	Mix	DR BoNT/A	0.2	140	398
3	072007.#00	20 (+/- 5)	243	4.8	DPPC	Mix	DR BoNT/A	0.2	3	546
4	072307.#00	20 (+/- 5)	243	4.8	DPPC	Mix	DR BoNT/A	0.2	45	474
5	072507.#00	20 (+/- 5)	243	4.8	DPPC	Mix	DR BoNT/A	0.2	65	350
6	072607.#01	20 (+/- 5)	243	4.8	DPPC	Mix	DR BoNT/A	0.2	35	491
7	082007.#00	20 (+/- 5)	243	4.8	DPPC	GT1b	DR BoNT/A	0.2	53	526
8	092607.#01	20 (+/- 5)	160	4.8	DPPC	Mix	DR BoNT/A	0.2	10	469
9	082907.#00	20 (+/- 5)	243	4.8	DPPC	Mix	Boiled DR BoNT/A	0.2	9	531
10	110607.#00	30 (+/- 1)	153	7.7	DPPC	Mix	BoNT/A HC	0.12	92	460
11	110907.#00	30 (+/- 1)	153	7.7	DPPC	Mix	BoNT/A HC	0.12	12	492
12	111207.#01	30 (+/- 1)	153	7.7	DPPC	Mix	BoNT/A HC	0.12	37	510
13	090407.#01	20 (+/- 5)	243	4.8	DPPC	Mix	BoNT/A HC	0.12	20	446
14	100207.#00	30 (+/- 1)	160	4.8	DPPC	Mix	BoNT/A HC	0.12	20	518
15	111407.#00	30 (+/- 1)	160	4.8	DPPC	Mix	BoNT/A HC	0.12	16	555
16	111007.#00	30 (+/- 1)	160	4.8	DPPC	Mix	BoNT/A HC	0.12	14	436
17	PRE082007.#00 UNRECORDED	20 (+/- 5)	243	4.8	DPPC	NONE	DR BoNT/A	0.2	0	Undetermined
18	083007.#03	20 (+/- 5)	243	4.8	DPPC	NONE	DR BoNT/A	0.2	0	435
19	100907.#00	30 (+/- 1)	160	4.8	DPPC	Mix	HCQ	0.2	3	520
20	072307 UNRECORDED	20 (+/- 5)	243	4.8	DPPC	Mix	HCQ	0.2	~3	Undetermined
21	101607.#01	30 (+/- 1)	160	4.8	DPPC	Mix	ALBUMIN	0.2	0	495
22		30 (+/- 1)	160	4.8	DPPC	Mix	ALBUMIN	10	0	502

Table 2. Raw listing of BoNT/A LB expansion parameters and results. Groupings found in figure12 are as follows: Bar#1-(1,2), Bar#2-(4-8), Bar#3-(10-12), Bar#4-(14-16), Bar#5-(17,18), Bar#6-(19,20), Bar#7-(21,22).

Bradley A. Strongin

2289 West 540 North   Provo, UT 84601   (801)375-7268
bradstrongin@yahoo.com

EDUCATION

- **MS, Physiology and Developmental Biology**, Brigham Young University, Provo UT, December 2007
- **BS, Applied Physics**, Brigham Young University, Provo UT 2005
  - Mathematics Minor

SKILLS

- Scientific Research
  - Atomic Force Microscopy (AFM)
  - Scanning Electron Microscopy (SEM)
  - Transmission Electron Microscopy (TEM)
  - Langmuir-Blodgett Trough Thin Film Deposition
  - Langmuir Lipid Monolayer Artificial Membrane Studies
- Bilingual: English/Spanish
- Microsoft Word, PowerPoint
- Scientific Writing
- Carpentry, End Mill, Wood and Metal Lathes

WORK / RELATED EXPERIENCE

- **Research Assistant**, Department of Physics & Astronomy and Department of Physiology & Developmental Biology 2002-2007

  Research Topics:
  - "Botulinum Neurotoxin Serotype A," 2005 - 2007
  - "The Influenza A M2 Proton Channel," 2002 – 2005

  Publication:
  - Hughes, T., **B. Strongin**, F. Gao, V. Vijayvergiya, D. Busath, and R. Davis (2004), AFM Visualization of Mobile Influenza A M2 Molecules in Planar Bilayers. Biophys. J. 87:311-322.

  Poster Presentations, Biophysical Society Annual Meetings
  - Co-authored, Miller, C. et al. "Constant-Pressure Expansion of Lipid-Ganglioside Monolayer by Botulinum Neurotoxin Serotype A: Does pH or Dithiothreitol Have More Impact?" **2007**
  - Co-authored, Swenson, R. et al. "Preliminary Structure, Function, and Modeling of the Botulinum Toxin Heavy Chain in Lipid Membranes." **2006**
  - Principal Investigator, **Strongin, B**. et al. "Atomic Force Microscope Imaging of Influenza M2 Proteins in Supported Planar Bilayers." **2005**

  Poster, American Physical Society March Meeting
  - Co-authored, Hughes, T. et al. "Bilayer Incorporated Influenza A M2 Single Molecule Time- Dependent AFM Studies." **2004**

- **Teaching Assistant**, Taught Principles of Physiology Lab, Brigham Young University, 2006 – 2007
  - 15 to 20-Minute Introductory Lectures. 9 class sections with 11 labs each (99 lectures)
- **Collaborating Scientist**, Los Alamos National Laboratory Neutron Reflectometry
  - 5 Combined Days of Training and Beam Time, June 2006

- 3 Days of Beam Time, August 2007
- **Patient Care Technician (PCT)**, Cardiovascular Unit, Utah Valley Regional Medical Center, 1 year 2001 - 2002
- **Financial Clerk** – Office Depot, 1 year 1998 - 1999
  - Performed Daily Internal Sales Audits

COMMUNITY SERVICE
- **Volunteer Representative** – The Church of Jesus Christ of Latter-day Saints, Guatemala, 2 years 1996 - 1998
- **Eagle Scout**, Boy Scouts of America 1995
  - Cub Scout Webelos Den Leader, 1 year 2006